

Evidence of angiogenesis and microvascular regression in autosomal-dominant polycystic kidney disease kidneys: A corrosion cast study

W Wei¹, V Popov², JA Walocha³, J Wen² and E Bello-Reuss^{1,4}

¹Department of Internal Medicine, University of Texas Medical Branch, Galveston, Texas, USA; ²Department of Pathology, University of Texas Medical Branch, Galveston, Texas, USA; ³Department of Anatomy, Collegium Medicum of Jagiellonian University, Cracow, Poland and ⁴Department of Neuroscience and Cell Biology, University of Texas Medical Branch, Galveston, Texas, USA

Autosomal-dominant polycystic kidney disease (ADPKD) accounts for about 10% of all cases of chronic renal failure requiring dialysis. The disease is characterized by proliferation of renal epithelial cells and formation of cysts that expand over years and replace the normal parenchyma of the kidney. As the cysts grow, the volume of the kidney can increase by more than 10-fold, implying that remodeling and expansion of the vasculature must occur to provide oxygenation and nutrition to the cyst cells. Our previous studies support the notion that there is angiogenesis in ADPKD. We report here results from resin casting of ADPKD kidneys vasculature. In this study, the corrosion-casting method was used in conjunction with scanning electron microscopy to study the vascular architecture and the evidence for angiogenesis in ADPKD kidneys. We found a well-defined vascular network around the cysts forming a 'vascular capsule' somewhat similar to that described in avascular leiomyomata. We also found that the normal vascular architecture is lost and replaced by an assortment of capillaries of larger size than those in the normal kidney, mixed with flattened and spiral arterioles, damaged glomeruli, and atresic venules, indicative of regression of the microvasculature. In the same areas, there was capillary sprouting, considered the hallmark of angiogenesis. The present study documents regression changes of the vasculature and confirms the existence of angiogenesis in ADPKD kidneys, and suggests the use of inhibitors of angiogenesis as a possible avenue for the treatment of the disease.

Kidney International (2006) **70**, 1261–1268. doi:10.1038/sj.ki.5001725; published online 2 August 2006

KEYWORDS: genetic renal disease; polycystic kidney disease; renal pathology; end-stage kidney disease

Correspondence: E Bello-Reuss, Department of Internal Medicine, Division of Nephrology, University of Texas Medical Branch, 4.200 John Sealy Annex, 301 University Boulevard, Galveston, Texas 77555-0562, USA.
E-mail: ebellore@utmb.edu

Received 10 January 2006; revised 20 April 2006; accepted 23 May 2006; published online 2 August 2006

Autosomal-dominant polycystic kidney disease (ADPKD) is the most frequent cause of end-stage renal disease secondary to a genetic disorder, accounting for about 10% of all cases of chronic renal failure requiring dialysis or transplantation.¹ It is caused by the mutation of either the *PKD-1* or the *PKD-2* genes, which encode polycystin-1 and -2, respectively.^{2,3} The disease is characterized by the proliferation of renal epithelial cells forming cysts that expand over years and replace the normal parenchyma of the kidney. Polycystic kidney disease has been considered akin to a benign tumor.⁴ As the cysts grow, the volume of the kidney can increase by more than 10-fold, implying that remodeling and expansion of the vasculature must occur to provide oxygenation and nutrition to the cyst cells. Our previous studies support the notion that there is angiogenesis in ADPKD despite the fact that in the past the renal vasculature in ADPKD, assessed by radiological and imaging techniques, has been described as 'attenuated'.^{5,6} We found that there is a rich vascular network around the cysts and evidence that angiogenesis, that is, the growth of new vessels from pre-existing ones, is a component of this disease.⁷ In that study, performed on kidneys removed from patients with ADPKD, we examined the morphology of the vasculature using conventional and fluorescein angiography, as well as 'ex vivo' preparations and immunostaining for factor VIII-related antigen. We found vascular malformations and evidence for vascular remodeling demonstrated by coexpression of matrix metalloproteinase 2 and integrin $\alpha_v\beta_3$ in vessels surrounding the cysts.⁷

The corrosion-casting technique has been recently revived and used, in conjunction with scanning electron microscopy for the morphological examination of normal tissues and tumors as an excellent method to study the quasi three-dimensional character of their vascularization.^{8–10} Vascular casting can provide evidence for microvascular remodeling and neof ormation based on the branching patterns and shapes of new growths from endothelial cells (furrows, bulges, sprouts). It allows – under ideal conditions – to assess the extent of the vascular proliferation and can be complementary to imaging methods.^{8,10–13} We report here

results from the casting of the vasculature of ADPKD kidneys removed from patients for medical reasons. In this study, the corrosion-casting method was used to study the alterations in kidney vascular architecture and the evidence of angiogenesis in ADPKD kidneys. We found a well-defined vascular network around the cysts forming a 'vascular capsule', somewhat similar to those described in leiomyomata.¹⁰ We also found that the normal vascular architecture is lost and replaced by an assortment of capillaries of larger size than those in the normal kidney, mixed with flattened and spiral arterioles, damaged glomeruli, and atresic venules, indicative of regression of the microvasculature. In the same areas, there was capillary sprouting, considered the hallmark of angiogenesis. The possibility that the angiogenesis observed is secondary to nonspecific progression of the renal disease is addressed in the Discussion. The present study documents regression changes of the vasculature and confirms the existence of angiogenesis in ADPKD kidneys, suggesting the use of inhibitors of angiogenesis as an avenue for the treatment of the disease.

RESULTS

Four normal kidneys, rejected for transplantation, were studied. The mean age of the kidney donors was 47.5 years, range 19–63 years (three men, one woman). The macroscopic appearance of one of the kidneys (normal kidney no. 2), injected from the renal artery, is shown in Figure 1a. This kidney measured $9 \times 4.5 \times 4 \text{ cm}^3$. In the normal kidneys, the resin filled the whole vascular bed and the casts reproduced the normal shape of the organ. Casting was made in seven ADPKD kidneys, all from end-stage renal disease patients (Chronic Kidney Disease Stage V) either on chronic dialysis or previous recipients of a kidney transplant and scanning electron microscopy was performed in five of them. The mean age of the ADPKD patients was 50.3 years, range 40–55 years (four women, three men; not significantly different from the age of normal kidney donors). Three were on dialysis (1 month, 2 months, and 5 years, respectively) and three were transplant recipients; there was no information on the last patient. The macroscopic appearance of ADPKD kidneys was not different from that reported previously.⁷ The ADPKD kidney size ranged from $19 \times 8.5 \times 5$ to $32 \times 20 \times 20 \text{ cm}^3$. The normal kidney parenchyma was replaced by cysts of variable sizes containing clear or dark fluid, the latter denoting bleeding inside the cysts. Macroscopically, there were no areas of recognizable normal structure. Because of the size of the kidneys, only one branch of the segmental anterior artery was cannulated for injection, as described in Materials and Methods. Figure 1b shows the macroscopic appearance of a cast from a segment, measuring $15.0 \times 9.4 \times 4.0 \text{ cm}^3$, of an ADPKD kidney (ADPKD kidney no. 6; Nikon D1 × camera, Nikon Inc., Melville, NY, USA), demonstrating total loss of the normal structure. Resin-filled vessels surround the cysts and reproduce their shape, revealing a network of small and larger vessels displaced by the cysts (Figure 1c).

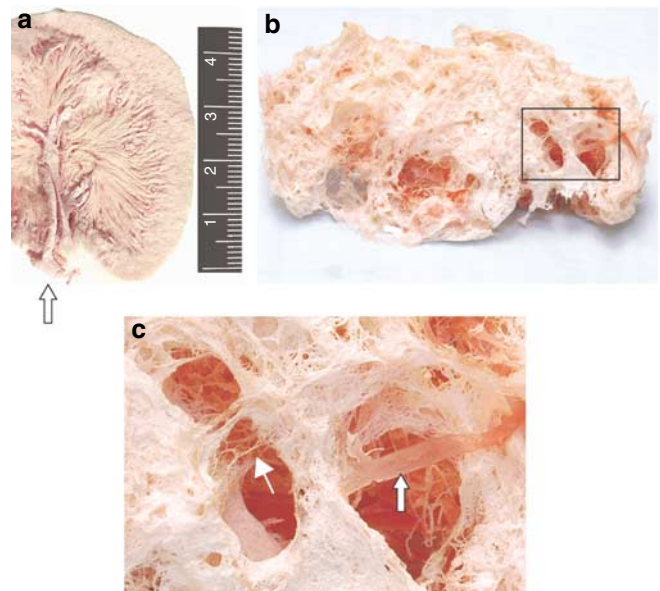


Figure 1 | Macroscopic images of normal and ADPKD kidneys. (a) Corrosion cast of a normal kidney demonstrating the regular distribution of the blood vessels. The cast reproduces the shape of the organ. (Arrow) Cannulated renal artery. (b) Cast of a segment (measuring $12.5 \times 5.3 \times 5.0 \text{ cm}^3$) from ADPKD kidney no. 6. Note the absence of normal kidney structure and the presence of avascular areas corresponding to spaces occupied by the cysts. These areas are surrounded by vasculature. Ruler between (a) and (b) in cm. (c) $\times 4$ enlargement of the rectangular area marked in panel b. The larger cyst that measures ~ 1 by 0.6 cm diameter (arrow) is crossed by a flattened vessel. White arrow indicates small vessels in an adjacent cyst (Nikon D1 × camera, Nikon Inc., USA).

Scanning electron microscopy further demonstrates the distortion of the microvasculature. Figure 2a–c shows the wall of a small cyst measuring $0.45 \times 0.30 \text{ mm}^2$ (ADPKD kidney no. 6) at progressively higher magnifications. An artery is displaced and bends following the contour of the cyst, acquiring a ribbon-like appearance on the left side of the cyst; flattened veins (Figure 2c) and the remnants of a glomerulus are visible. Figure 2d–f depicts a cyst from ADPKD kidney no. 7. An abnormal number of larger vessels ($40\text{--}70 \mu\text{m}$) are seen in the vicinity of the cyst cavity; at higher magnification, capillaries (ca. $5 \mu\text{m}$ diameter) are interspersed with larger vessels (ca. $25 \mu\text{m}$ diameter); capillary branching is sparse.

The distribution of diameters of the blood vessels in normal kidney cortex and ADPKD cyst walls is depicted in Figure 3 (all vessels measured: normal kidney, $n = 3534$; ADPKD kidneys, $n = 3052$). The mean vessel diameter in the cortex of the normal kidneys ($n = 4$) was significantly different from the mean diameter in ADPKD kidneys, 15.2 ± 0.1 vs $18.6 \pm 0.2 \mu\text{m}$, respectively (mean \pm s.e., $n = 5$, ADPKD kidneys); the t -statistic is 12.54 with $P < 0.0001$ (normal vs ADPKD kidneys). The variation of vessel diameter was also significantly different between normal and ADPKD kidneys; the F -statistic is 4.16, $P < 0.0001$; normal vs ADPKD. Finally, the distribution of vessel diameter was significantly different between control and experimental

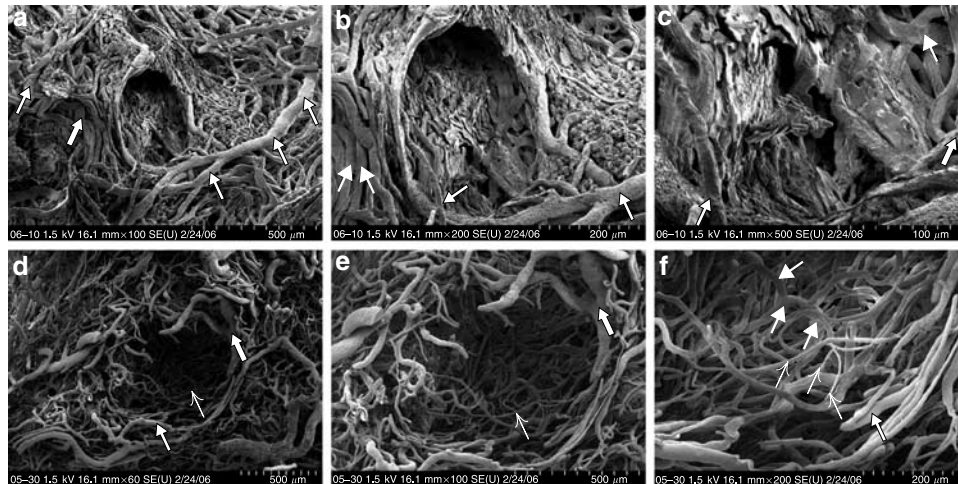


Figure 2 | Scanning electron microscopy of ADPKD cyst walls. (a–c) The upper half of a small cyst (from ADPKD kidney no. 6) measuring $\sim 0.45 \times 0.30 \text{ mm}^2$ was removed and the resulting cavity is shown at progressively higher magnifications in scanning electron microscopy. (a) The cyst in the center has grown into the native kidney parenchyma; the normal structures are not longer recognizable. Flattened veins are seen in a shallow cyst (left-side, thick arrow). Thin dark-edge arrows identify arteries (bar = $50 \mu\text{m}$ per division). (b) A branch of an artery (dark-edge arrow) curves up following the left-side contour of the cyst and has a ribbon-like appearance. Flattened veins in the shallow cyst on the left side are indicated by white arrows (bar = $20 \mu\text{m}$ per division). (c) Ribbon-like veins (white arrow), an arteriole (thick dark-edge arrow), and the oval imprint of an arteriole nucleus (thin dark-edge arrow) are shown, as well as the remnants of a damaged glomerulus on the right side of the nuclear imprint (bar = $10 \mu\text{m}$ per division). (d–f) Scanning electron microscopy of a cyst from ADPKD kidney no. 7 at progressively higher magnifications. The cyst top has been removed, at the bottom there is no recognizable normal kidney structure. (d) An artery (thick dark-edge arrow) on the right side follows the contour of the cyst. Numerous larger vessels ($40\text{--}70 \mu\text{m}$) are seen in the perimeter. The thin dark-edge arrow denotes an arteriole; the winged arrow marks a capillary (bar = $50 \mu\text{m}$ per division). (e) At higher magnification, small caliber capillaries (ca. $5 \mu\text{m}$; area around the winged arrow) are interspersed with larger vessels ($25 \mu\text{m}$). Capillary branching is sparse. Thick dark-edge arrow on the right marks an artery (bar = $50 \mu\text{m}$ per division). (f) High power of the lower right corner of (e). Dark-edge arrow: arteriole; white arrows: venules; winged arrows: capillaries. The vessels on the right-hand side are displaced, arching to conform to the cyst shape (bar = $20 \mu\text{m}$ per division).

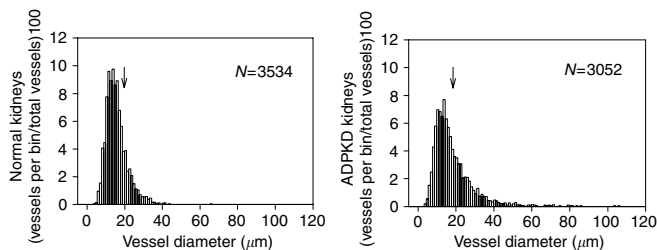


Figure 3 | Distribution of blood vessel diameters in normal kidney cortex (NK) and in ADPKD cyst walls (ADPKD). It is clear that there is a higher percentage of large vessels in the ADPKD kidneys; compare the two distributions above $20 \mu\text{m}$ diameter. Numbers of blood vessels indicated in the figure (N); four normal kidneys and five ADPKD kidneys were studied.

groups. The goodness-of-fit statistic is 1562.2 (degrees of freedom = 20) with $P < 0.0001$; normal vs ADPKD kidney vessels).¹⁴ The main difference between both histograms is the higher percentage of large vessels in the ADPKD kidneys (compare, in Figure 3, the two distributions above $20 \mu\text{m}$ diameter).

Under magnification by stereomicroscope, and also by scanning electron microscopy, areas with conglomerates of preserved glomeruli were noted (Figure 4a and b, from ADPKD kidneys nos. 1 and 3, respectively). For comparison, Figure 4c and d shows normal kidney cortex (normal kidney

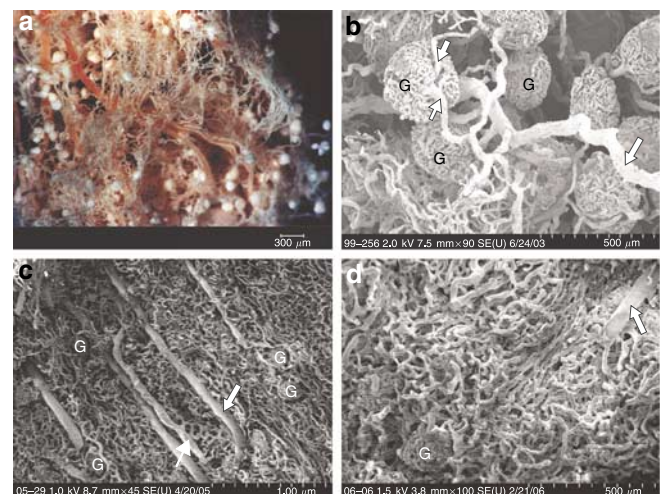


Figure 4 | Distribution of glomeruli and vessels in ADPKD and normal kidneys. (a) Stereomicroscopic and (b) scanning electron microscope microphotograph showing areas with conglomerates of preserved glomeruli recognizable as the white round structures in (a) (bar = $300 \mu\text{m}$) and marked G in (b) (bar = $50 \mu\text{m}$ per division; ADPKD kidneys nos. 2 and 3, respectively). Capillaries from the peritubular network are sparse, with diminished branching. (c, d) Normal kidney cortex (normal kidneys nos. 2 and 3, respectively) depicting the parallel array of interlobular arteries (dark-edge arrow), an interlobular vein (white arrow), and glomeruli (G). The peritubular capillary network homogeneously fills all the space between the other structures (c: Bar = $100 \mu\text{m}$ per division; d: bar = $50 \mu\text{m}$ per division).

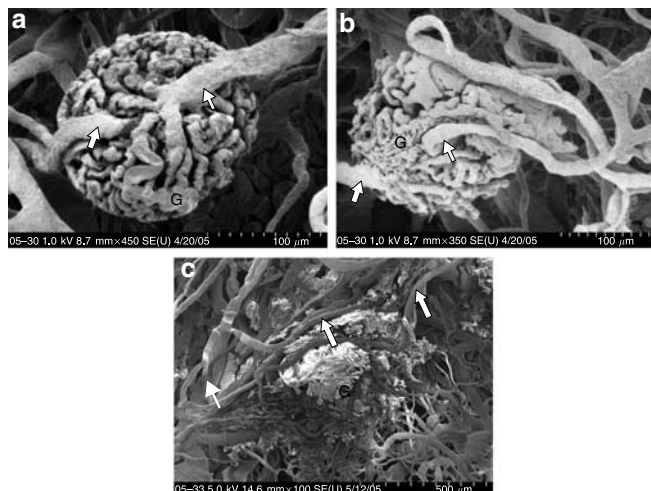


Figure 5 | Glomeruli exhibiting variable degree of damage (ADPKD kidneys nos. 6 and 7). G: glomeruli; thick arrow: afferent arteriole; thin arrow: efferent arteriole. (a) ADPKD remnant glomerulus showing afferent and efferent arterioles (bar = 10 μ m per division). (b) A more damaged glomerulus with its afferent and efferent arterioles still identifiable (bar = 10 μ m per division). (c) A glomerulus with flattened capillaries is shown at the center and a flattened vein (white arrow) is seen at the left side (dark-edge arrows), arteries (Bar = 50 μ m per division).



Figure 6 | A cyst wall with corkscrew-shaped arteriole (dark-edge arrow; from ADPKD kidney no. 7) and flattened smaller arterioles with assorted shapes in the background. Winged arrow, capillary (bar = 50 μ m per division).

nos. 2 and 3, respectively) illustrating the parallel array of interlobular arterioles and neighboring glomeruli. The rest of the field is completely occupied by the peritubular capillary network. In ADPKD kidneys, the glomeruli exhibited variable degree of damage, and occasionally both afferent and efferent arterioles were recognizable (Figure 5a-c; ADPKD kidney nos. 6 and 7). Thus, scanning electron microscopy studies of the microvascular network of ADPKD kidneys demonstrate the coexistence of remnant and damaged glomeruli and, frequently, flattened and corkscrew-shaped arterioles (Figure 6). In the damaged glomeruli (Figure 7) as well as in atresic veins (Figure 8), vascular sprouts were found. Some damaged glomeruli exhibited small perforations of the capillaries, suggesting intussusceptive growth (Fig-

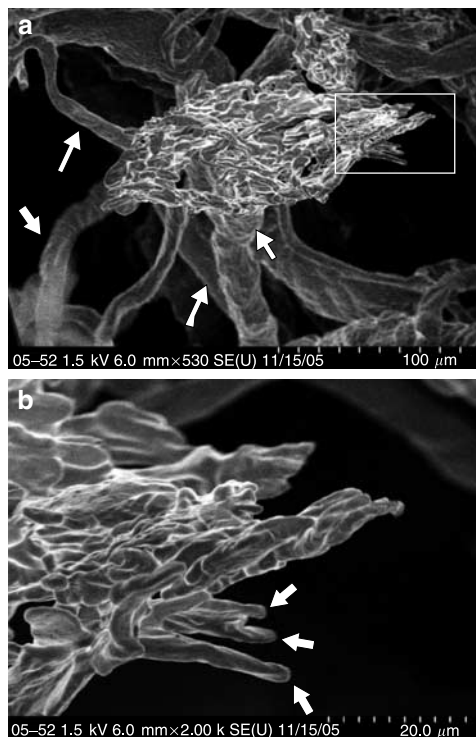


Figure 7 | Capillary sprouting in an ADPKD glomerulus. (a) Severely damaged glomerulus (ADPKD kidney no. 7). Afferent (short thick arrow) and efferent (short thin arrow) arterioles. Few arterioles are seen in the background surrounding the glomerular area (long dark-edge arrows) (bar = 10 μ m per division). (b) High magnification of boxed area in (a) showing an atresic glomerulus with vascular sprouts originating in the three lower capillaries (arrows) (bar = 2 μ m per division).

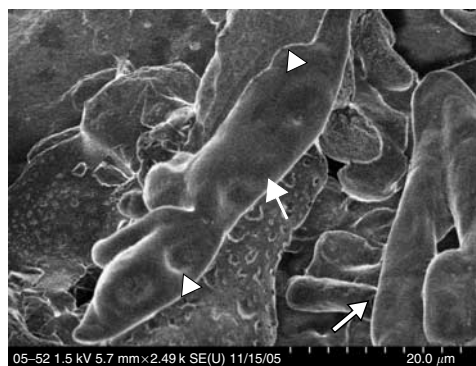


Figure 8 | A venule (white arrow; from ADPKD kidney no. 7) with dead ending tributaries typical of vascular atresia. Note small sprouts on the surface of the vessel (arrowheads). On the right side, an arteriole is visible (dark-edge arrow) (bar = 2 μ m per division).

ure 9); however, incomplete filling could give a similar appearance. The glomerular and venular damage denote regression of the microvasculature, whereas the vascular sprouts are indicative of angiogenesis.^{8,13}

At high-power scanning electron microscopy, we regularly observed blood vessels surrounding the removed cysts (Figure 10). These vessels were heterogeneous in size and

lacked the orderly appearance of the microvasculature typical of the normal kidney. Arterioles were identified by the characteristic imprints of the nuclei of endothelial cells (oval in shape and sharply contoured), located along the longitudinal axis of the vessels (Figure 10a). Vascular sprouts growing from a venule, unambiguously denoting angiogenesis, are shown in Figure 10b. Venules were identified by their characteristic endothelial cell nuclear imprints (superficial, poorly contoured, and irregularly dispersed through the surface), as seen also in Figure 10c and e.

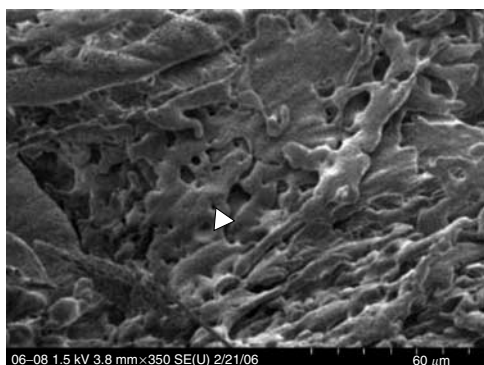


Figure 9 | Scanning electron microscopy of a cyst wall (from ADPKD kidney no. 6) showing capillaries with small holes (1–3 μm) like the one marked by the arrowhead. The small holes could correspond to intussusceptive forms of angiogenesis, but a similar aspect can be the result of incomplete vascular filling by the resin (bar = 10 μm per division).

DISCUSSION

Corrosion casting combined with scanning electron microscopy has been recently used to study blood vessels in normal tissues and tumors, including the kidney (reviewed by Konerding *et al.*,¹¹ Dietrich and Splechtna,¹² and McDonald and Choyke¹³). The method has allowed the identification of elements indicative of angiogenesis. These are the sprouting of capillaries from pre-existing vessels, of which the bulges and sprouts identified in Figures 7 and 8 are examples,^{11,15} and growth by intussusception, in which endothelial cell columns split a capillary to originate two or more, as described in the development of rat pulmonary microcirculation and in the normal and pathological kidney.^{16–18} Despite the fact that we found some glomerular capillaries with small holes (ca. 1–3 μm diameter), this finding always occurred in glomeruli with advanced damage and we cannot rule out that they are an artifact owing to insufficient filling by the resin. Demonstration of intussusceptive capillary growth requires ultrastructural demonstration of pillars and serial reconstruction,¹⁶ a study that will be difficult to perform in ADPKD kidneys given the heterogeneity of the glomerular lesions, and not possible in the fragments mounted for scanning electron microscopy.

In contrast to the vascularization of large solid tumors, the blood vessels in ADPKD do not penetrate the cysts, forming instead a pericyclic ‘vascular capsule’, resembling the appearance of small avascular leiomyomata.¹⁰ Morphometric analysis demonstrated that the diameter of the capillaries surrounding the cysts was significantly larger than that of the

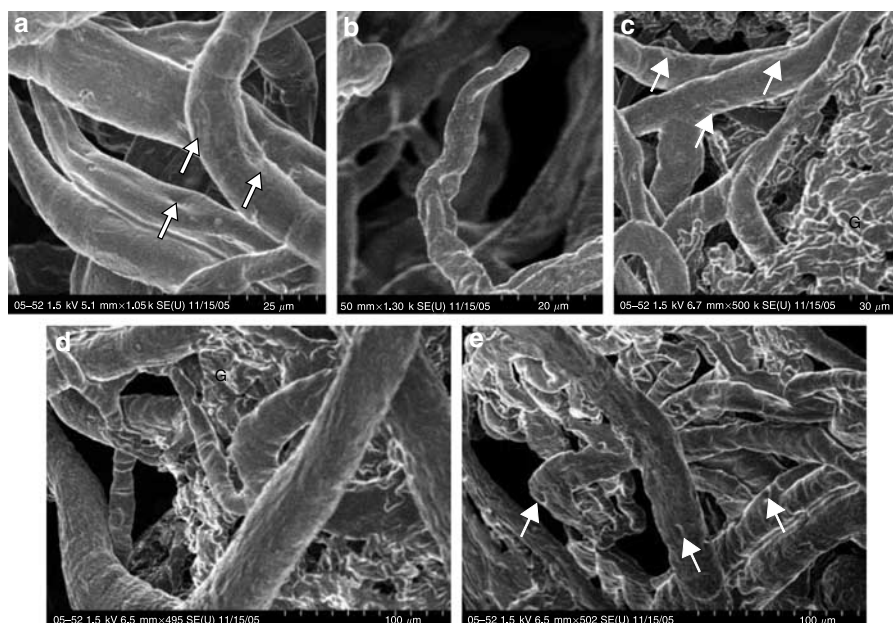


Figure 10 | Scanning electron microscopy of ADPKD kidney vasculature (from ADPKD kidney no. 7). (a) High-power microphotograph of a cyst wall showing the characteristic imprints of nuclei of endothelial cells located along the longitudinal axis of the vessel, oval in shape and sharply contoured identify arterioles (dark-edge arrows) (bar = 5 μm per division). (b) Vascular sprout growing from a venule (bar = 4 μm per division). (c) Left side, venules with characteristic nuclei imprints (white arrows) (bar = 10 μm per division). Right side, damaged glomerulus (G). (d) Arterioles supplying a damaged glomerular tuft (G) (bar = 10 μm per division). (e) Network of venules with visible nuclei imprints (white arrows). In the right lower corner surface, irregularities denote poor corrosion on the surface of the vascular cast (bar = 10 μm per division).

cortical capillaries of the normal kidney. The mean capillary vessel diameters in ADPKD kidneys, although larger than those of normal kidneys, are distinctly smaller than the ones reported in human primary renal clear cell carcinoma.^{19,20} ADPKD cysts are benign in nature, the basement membrane is preserved and, at least in the kidneys, in renal failure, there are fewer proliferative vessels (sprouting) than those reported in malignant tumors.²¹ Our studies demonstrate the changes in the architecture of the kidney and document the presence of flattened large vessels and of glomerular capillaries as well as the disappearance of the cortical capillary network. Changes suggesting compression had been invoked as causative or contributory to the evolution of ADPKD kidneys to renal failure,^{5,22,23} but there is not yet a clear understanding of the determinant mechanisms of the glomerular damage, interstitial fibrosis, and tubule transdifferentiation involved in such progression (see below).

Our studies revealed corrosion-cast shapes compatible with those reported in the literature as corresponding to angiogenesis in other tissues and tumors. Capillary shapes consistent with angiogenesis were found in several areas and confirm our previous findings.⁷ We have also found that the angiogenic factors vascular endothelial growth factor, platelet-derived growth factor, and interleukin-8 are secreted by the cyst cells, which also express the corresponding receptors (E Bello-Reuss, W Wei, W Hui-Qun, unpublished observations. *Am Soc Nephrol* 2005; **16**:586A).

At birth, patients with ADPKD have kidneys that are normal both morphologically and functionally; cyst growth progressively diminishes renal function because the normal parenchyma is replaced by cysts and interstitial fibrosis. The loss of renal function by age 50–60 years makes life unsustainable for ADPKD patients without dialysis or renal transplant. Thus, the evolution of the disease comprises (1) the development of cysts and their growth for which vessel elongation and neovascularization are favored by the secretion of angiogenic factors by the cyst cells and (2) the demise of the initially normal parenchyma, a process that is not well understood.

The initial response to a decrease in nephrons is a short-lived hypertrophy of the remnant glomeruli followed by apoptosis and progressive loss of endothelium; a similar loss of capillaries has been reported in interstitial nephritis. The loss of capillaries correlates with the severity of glomerulosclerosis and interstitial fibrosis (for a review, see Kang *et al.*²⁴). Recent studies suggest that chronic tubulointerstitial hypoxia is the common pathway to renal failure and that advanced tubulointerstitial damage results in loss of peritubular capillaries. This causes tubule cell hypoxia leading to apoptosis and transdifferentiation of tubule cells into myofibroblasts, which, in turn causes fibrosis (for a review, see Nangaku *et al.*²⁵). Ischemia has been postulated in the progression to chronic renal failure in focal segmental glomerulosclerosis, in the chronic interstitial scarring of chronic rejection, in age-associated kidney disease and in the remnant kidney model.²⁶ There is experimental evidence

demonstrating impaired angiogenesis in a rat model of progressive renal failure and it has been shown that administration of vascular endothelial growth factor reduces the fibrosis and stabilizes the renal function.²⁷ Thus, the available information indicates that forms of chronic renal failure other than ADPKD are not accompanied by angiogenesis.

The mechanism of the progression of the damage of ADPKD kidneys remains obscure. Persistence of relatively normal parenchyma between cysts, persistence of normal glomeruli, and the disappearance of the microvascular bed have been described.^{28,29} This is concurrent with the observation of flattened glomeruli attached to the cyst walls, which remain permeant to contrast material.³⁰ Neither proteinuria nor glomerulitis-initiated damage seems to play a role in ADPKD progression to renal failure. Indeed, in chronic renal failure of all origins, interstitial fibrosis correlates better with the decrease in glomerular filtration rate than the number of glomeruli with normal appearance in renal biopsies. Interstitial fibrosis can be initiated by physical factors or by an inflammatory response triggering the release of cytokines and growth factors. Presently, this is an area of intense investigation (for a review, see Razzaque and Taguchi³¹). Franz *et al.*²² suggested that compression of the vasculature could explain the progressive damage to the native normal nephrons in ADPKD; earlier studies by Ritter and Baehr⁵ indicated that the atrophic, sclerosed parenchyma between cysts resembles the contracted kidney of hypertension, noting that ‘the interlobar and interlobular vessels were elongated due to stretching’. The microscopic observation of sclerosed glomeruli and tubule atrophy suggested that ischemia played a role in the progression to renal failure (reviewed by Ecker and Schrier²³).

Taken together with our previous results,⁷ our findings suggest the existence of an autocrine/paracrine mechanism for cyst growth and angiogenesis. Teleologically, angiogenesis in ADPKD kidneys can be understood as a phenomenon favoring cyst cell proliferation and cyst growth. The cysts progressively replace the native renal tissue, conducting to renal failure. The mechanism of the progression of chronic kidney disease remains unclear, likely resulting from multifactorial influences including ischemia, hypertension, cytokine release by cyst cells, and perhaps others yet to be determined. As inhibition of cyclic adenosine monophosphate-mediated cyst growth has an important role in the preservation of renal function in polycystic kidney mice,^{32,33} it is possible that inhibition of angiogenic factors may prove to be a useful approach, by itself or complementary, for the treatment of the disease.

MATERIALS AND METHODS

Seven ADPKD kidneys, removed surgically because of medical indications from patients with end-stage renal disease and donated for research to the Polycystic Kidney Research Foundation, were used. Four normal kidneys, rejected for transplantation and donated for research, were also studied (the investigators were not involved in the medical decision making; the protocol was approved by the

Internal Review Board, University of Texas Medical Branch). Kidneys were perfused with lactate-Ringer's solution containing 1000 U heparin/l, followed (in 3/7 cases) by infusion of 0.66% paraformaldehyde and 0.08% glutaraldehyde in 0.2 M cacodylate buffer, pH 7.4. The normal kidneys were removed connected to a flap of aorta (because of the intention of transplanting them), thus the renal artery was readily available for cannulation and entire kidneys were injected with casting material. In contrast, the ADPKD kidneys were removed by sectioning the renal artery or arteries close to the hilum and, because of large sizes of the kidneys, only one branch of the segmental anterior artery was cannulated and about 60–80 ml of the casting material was infused manually as per the manufacturer's recommendations (Mercor-Jap, Vilene Co., Ladd Research Industries, Williston, VT, USA). The perfused section of the kidney was removed and, after polymerization of the casting material, the soft tissues were digested by repeated washes in 10% KOH at 37–50°C for about 10 days, with distilled water washes every other day. When the soft tissues were completely removed, the casts were washed exhaustively with distilled water, cleaned with formic acid (5%), washed again, and dried over a nylon mesh placed over a perforated porcelain plate inside a vacuum desiccator containing drierite. Some dry specimens were immersed in a mixture of polyethylene glycols, as recommended by Walocha *et al.*,³⁴ in order to avoid damage to the surface and deep regions of the specimen. Briefly, a mixture of 1:20 (w/w) polyethylene glycols 600:2000 (Fluka BioChemical, distributed by Sigma Aldrich, St Louis, MO, USA) was prepared and placed in a water bath at 55–60°C until solubilized. Samples were immersed in the mixture, which solidifies at room temperature; the included samples were trimmed to the desired orientation and size. Polyethylene glycols were removed by immersion in distilled water in a plastic double bath. The sample was placed inside a bottom-perforated container, bathed in water, and vigorously stirred. After polyethylene glycols were removed, the sample was transferred to a vacuum desiccator. Dried casts were examined with a stereomicroscope and representative areas were selected for scanning electron microscopy. Macroscopic samples were photographed with a Nikon D1 × digital camera, saved, and stored for image processing.

For scanning electron microscopy, pieces of casts were cut out with a sharp razor blade, mounted on specimen stubs using double-coated adhesive tape with a drop of silver paint or, in large samples, using Silver Adhesive 503 (Electron Microscopy Sciences, Hatfield, PA, USA), and then sputter-coated with iridium for 40 s at 20 mA in an Emitech K575X turbo sputter coater (Emitech, Houston, TX, USA). The samples were examined in a Hitachi S-4700 field emission scanning electron microscope (Hitachi High Technologies America Inc., Electron Microscope Division Headquarters, Pleasanton, CA, USA) at 2 kV and emission current 10 mA.

Identification of the vessels was carried out by one of the authors (JAW) according to the vessel diameter and shape of endothelial nuclei; budding and sprouting were considered indicative of angiogenesis.¹¹

Image processing and analysis of the vessel diameter data were performed with a computer (Dell Computer Corporation, Round Rock, TX, USA) equipped with image processing software (Adobe Photoshop; Adobe Systems, Mountain View, CA, USA), using the UTHSCSA *Image Tool* program developed at the University of Texas Health Science Center at San Antonio, San Antonio, TX, USA by Wilcox *et al.* and available in the Internet at <http://www.uthscsa.edu/dig/itdesc.html>.³⁵ Normal kidney vessels numbers and diameters were measured from images collected at ×100 magnification,

projected on a 20.5 × 14 cm² screen, in 94 squares from the corners of images divided in nine squares. Vessels were measured in 68 corner squares of ×100, ×350, and ×700 images from ADPKD kidneys. Results are reported from five ADPKD and four normal kidneys. The total studied area was 16.22 mm² in control and 12.82 mm² in ADPKD kidneys.

Statistical analysis

The data analysis for this paper was generated using SAS software version 9.1 (Copyright, SAS Institute Inc., Cary, NC, USA). Data are presented as mean ± s.e., Student's *t*-test, F-statistics, and goodness-to-fit analysis were used to compare the significance of the differences between vessel diameters from normal and ADPKD kidneys. A value of *P* < 0.05 was taken to indicate a significant difference.

ACKNOWLEDGMENTS

We thank Professor Adam J Miodonski (SEM Laboratory, Laryngology Clinic of Collegium Medicum, Jagiellonian University, Cracow, Poland) for help in the evaluation of SEM images and Professor Luis Reuss (Department of Neuroscience and Cell Biology, University of Texas Medical Branch, Galveston, TX, USA) for advice and review of a preliminary version of this article. The statistical help of Dr Yong-Fang Kuo (Department of Internal Medicine and Sealy Center on Aging, University of Texas Medical Branch, Galveston, TX, USA) is gratefully acknowledged. This study was partially supported by grants from the Polycystic Kidney Disease Foundation and the American Heart Association, Texas Affiliate to E Bello-Reuss and by funds from the Department of Internal Medicine, School of Medicine, UTMB, Galveston, TX, USA.

REFERENCES

- Gabow PA, Johnson AM, Kaehny WD *et al.* Factors affecting the progression of renal disease in autosomal-dominant polycystic kidney disease. *Kidney Int* 1992; **41**: 1311–1319.
- International PKD Consortium. Polycystic kidney disease: the complete structure of the PKD1 gene and its protein. *Cell* 1995; **81**: 289–298.
- Mochizuki T, Wu G, Hayashi T *et al.* PKD2, a gene for polycystic kidney disease that encodes an integral membrane protein. *Science* 1996; **272**: 1339–1342.
- Grantham JJ, Calvet JP. Polycystic kidney disease: in danger of being X-rated? *Proc Natl Acad Sci USA* 2001; **98**: 790–792.
- Ritter S, Baehr G. The arterial supply of the congenital polycystic kidney and its relation to the clinical picture. *J Urol* 1929; **21**: 583–592.
- Schacht F. Hypertension in cases of congenital polycystic kidney. *Arch Intern Med* 1931; **47**: 500–509.
- Bello-Reuss E, Holubec K, Rajaraman S. Angiogenesis in autosomal dominant polycystic disease. *Kidney Int* 2001; **60**: 37–45.
- Grunt TW, Lametschwandtner A, Karrer K. The characteristic structural features of the blood vessels of the Lewis lung carcinoma (a light microscopic and scanning electron microscopic study). *Scan Electron Microsc* 1986; **2**: 575–589.
- Casellas D, Mimran A. Shunting in renal microvasculature of the rat: a scanning microscopy study of corrosion casts. *Anat Rec* 1981; **201**: 237–248.
- Walocha JA, Litwin JA, Miodonski AJ. Vascular system of intramural leiomyomata revealed by corrosion casting and scanning electron microscopy. *Hum Reprod* 2003; **18**: 1088–1093.
- Konerding MA, Miodonski AJ, Lammetschwandtner A. Microvascular corrosion casting in the study of tumor vascularity: a review. *Scan Microsc* 1995; **9**: 1233–1244.
- Dietrich H, Splechtna H. Kidney structure investigation using scanning electron microscopy of corrosion casts – a state of the art review. *Scan Microsc* 1990; **4**: 943–956.
- McDonald DM, Choyke PL. Imaging of angiogenesis from microscope to clinic. *Nat Med* 2003; **9**: 714–725.
- Rosner B. *Fundamentals of Biostatistics*. 3rd edn. PWS-KENT Publishing Company: Boston, MA, 1990.

15. Jiang JY, Macchiarelli G, Tzang BK, Sato E. Capillary angiogenesis and degeneration in bovine ovarian antral follicles. *Reproduction* 2003; **125**: 211–223.
16. Notoya M, Shinosaki T, Kobayashi T *et al.* Intussusceptive capillary growth is required for glomerular repair in rat Thy-1.1 nephritis. *Kidney Int* 2003; **63**: 1365–1373.
17. Burri PH, Tarek MR. A novel mechanism of capillary growth in the rat pulmonary microcirculation. *Anat Record* 1990; **228**: 35–45.
18. Patan S, Alvarez MJ, Schittny JC, Burri PH. Intussusceptive microvascular growth: a common alternative to capillary sprouting. *Arch Histol Cytol* 1992; **55**(Suppl): 65–75.
19. Konerding MA, Malkusch W, Klapthor B *et al.* Evidence for characteristic vascular patterns in solid tumours: quantitative studies using corrosion casts. *Br J Cancer* 1999; **80**: 724–732.
20. Drevs J, Muller-Driver R, Wittig C *et al.* PTK787/ZK 222584, a specific vascular endothelial growth factor-receptor tyrosine kinase inhibitor, affects the anatomy of the tumor vascular bed and the functional vascular properties as detected by dynamic enhanced magnetic resonance imaging. *Cancer Res* 2002; **62**: 4015–4022.
21. Cameron IL, Short N, Sun L, Hardman EW. Endothelial cell pseudopods and angiogenesis of breast cancer tumors. *Cancer Cell Int* 2005; **5**: 17.
22. Franz KA, Reubi FC. Rate of functional deterioration in polycystic kidney disease. *Kidney Int* 1983; **23**: 526–529.
23. Ecker T, Schrier R. Hypertension in autosomal-dominant polycystic kidney disease: early occurrence and unique aspects. *J Am Soc Nephrol* 2001; **12**: 194–200.
24. Kang D-H, Kanellis J, Hugo C *et al.* Role of the microvascular endothelium in progressive renal disease. *J Am Soc Nephrol* 2002; **13**: 806–816.
25. Nangaku M. Chronic hypoxia and tubulointerstitial injury: a final common pathway to end-stage renal failure. *J Am Soc Nephrol* 2006; **17**: 17–25.
26. Kang D-H, Johnson RJ. Vascular endothelial growth factor: a new player in the pathogenesis of renal fibrosis. *Curr Opin Nephrol Hypertens* 2003; **12**: 43–49.
27. Kang D-H, Hughes J, Mazall M *et al.* Impaired angiogenesis in the remnant kidney model: II. Vascular endothelial growth factor reduces the renal fibrosis and stabilizes the renal function. *J Am Soc Nephrol* 2001; **12**: 1448–1457.
28. Zeier M, Fehrenbach P, Geb S *et al.* Renal histology in polycystic kidney disease with incipient and advanced renal failure. *Kidney Int* 1992; **42**: 1259–1265.
29. Reynes M, Diebold J, Camillere JP, Delarue J. Vascularization of polycystic kidneys in adults studied by the method of vascular injections. *Ann Anat Pathol (Paris)* 1969; **14**: 407–418.
30. Lund FB. Rovsing's operation for congenital cystic disease. *J Am Med Assoc* 1914; **63**: 1083–1089.
31. Razzaque MS, Taguchi T. Cellular and molecular events leading to renal tubulointerstitial fibrosis. *Med Electron Microscop* 2002; **35**: 68–70.
32. Gattone VH, Wang X, Harris PC, Torres VE. Inhibition of renal cystic disease development and progression by a vasopressin V₂ receptor antagonist. *Nat Med* 2003; **9**: 1223–1326.
33. Torres VE, Wang X, Qian Q *et al.* Effective treatment of an orthologous model of autosomal dominant polycystic kidney disease. *Nat Med* 2004; **10**: 363–364.
34. Walocha JA, Miodonski AJ, Nowogrodzka-Zagorska M *et al.* Application of a mixture of glycol polyethylenes for the preparation of microcorrosion casts – an observation. *Folia Morphol* 2002; **61**: 313–316.
35. Russ JC. *The image processing handbook*, 2nd edn. CRC Press: Boca Raton, FL, 1995.